Letters

Universal High-Frequency-Link Characterization and Practical Fundamental-Optimal Strategy for Dual-Active-Bridge DC-DC Converter Under PWM Plus Phase-Shift Control

Biao Zhao, *Member, IEEE*, Qiang Song, *Member, IEEE*, Wenhua Liu, Guowei Liu, and Yuming Zhao

***Abstract*—This letter first develops a universal steady-state model to simply and accurately describe the analytical expressions for the high-frequency-link (HFL) electrical quantities of isolated dual-active-bridge (DAB) dc–dc converter under PWM plus phase-shift control. Second, a universal reactive power interaction among the HFL electrical quantities is present; using this interaction, the circulating current characteristic of DAB can be described accurately by HFL power factor. On this basis, a practical HFL fundamental-optimal strategy is proposed to decrease the circulating current and increase the efficiency. At last, experimental results verify the correctness of the universal model and the effectiveness of the fundamental-optimal strategy.**

***Index Terms*—DC–DC converter, dual-active-bridge, high-frequency link, phase shift, pulse-width modulation.**

I. Introduction

In high-frequency (HF) isolated dual-active-bridge (DAB) dc–dc converter single-phase-shift (SPS) control is the simplest and most widely used control method [1]–[4]. However, because the power transmission depends on the transformer's leakage inductor and the HF square waves in high-frequency link (HFL), the circulating power will be very great when the voltage amplitude of two sides of the transformer is not matched, then the power loss becomes much higher and its efficiency is greatly reduced in practice [5]–[6].

In order to solve the aforementioned problem, PWM plus phase-shift (PPS) control is an effective method, such as extended-phase-shift (EPS) proposed in [7], dual-phase-shift (DPS) proposed in [8], and triple-phase-shift and hybrid-phase-shift proposed in [9]–[11]. What all of these PS control methods have in common is that the cross-connected switch pairs in two full-bridges are switched with an inner phase-shift (PS) angle, then the HFL voltage becomes three-level wave from the square wave, and the circulating power can be decreased.

Manuscript received April 13, 2015; accepted April 28, 2015. Date of publication May 7, 2015; date of current version August 21, 2015. This work was supported by the National High Technology Research and Development (863) Program of China under Grant 2013AA050104. (*Coresponding author: Qiang Song.*)

B. Zhao, Q. Song, and W. Liu are with the Department of Electrical Engineering, Tsinghua University, Beijing 100084, China (e-mail: zhaobiao@tsinghua.edu.cn; songqiang@tsinghua.edu.cn; liuwenh@tsinghua.edu.cn).

G. Liu and Y. Zhao are with the Shenzhen Power Supply Corporation, Shenzhen 518048, China (e-mail: liulgw@yeah.net; zhaoym97@sina.com).

Color versions of one or more of the figures in this paper are available online at http://ieeexplore.ieee.org.

Digital Object Identifier 10.1109/TPEL.2015.2430934

In order to explain the essence of the PPS controls for the improvement of the circulating current, the concept of the reactive power was employed in literatures [8] and [12]. Based on the definition, the reactive power is caused by the PS between the HFL voltages, but in fact, the circulating current is essentially caused by the amplitude mismatch between the HFL voltages. Therefore, the physical significance of the reactive power defined in the previous literatures is not clear, and the built analytic model has no universality, which cannot be used to explain the improve essence of the PPS controls.

In addition, the HFL electrical quantities of PPS methods were still modeled by the traditional piecewise linear method used in SPS [1]–[12]. Due to the increase of the adjustable control variables, the established models are different with different time intervals, different operation states, and different PPS methods, the models are very complex and the universality is low. It is hard and confusing to be used for the parameters calculation and design by engineers.

Moreover, in order to achieve the optimization operation of PPS control, it needs to select an optimal combination of the multiple control variables for PPS controls. The optimal methods were proposed based on a global optimal model for the efficiency in the literatures [13] and [14]. Although the method can achieve an optimal solution in theory, but as the global piecewise linear model is very complex, the optimal procedure is hard to perform in practice, especially the online accuracy is low for different conditions.

To address the above issues, this letter develops a universal model to describe the analytical expressions for the HFL electrical quantities of DAB, and presents a universal reactive power interaction among the HFL electrical quantities. On this basis, a practical HFL fundamental-optimal control strategy is proposed to decrease the circulating current and increase the efficiency.

II. Universal HFL Analytical Characterization

A. General Description for PPS control

During the steady state, the DAB can be equivalent to two high-frequency ac sources connected in both sides of an inductor, as shown in Fig. 1(a). In Fig. 1(a), L is the sum of the series inductance and leakage inductance of the high-frequency transformer; V_1 and V_2 are the dc terminal voltages of bridges H_1 and H_2, respectively; v_{h1} and v_{h2} are the HFL voltages of bridges

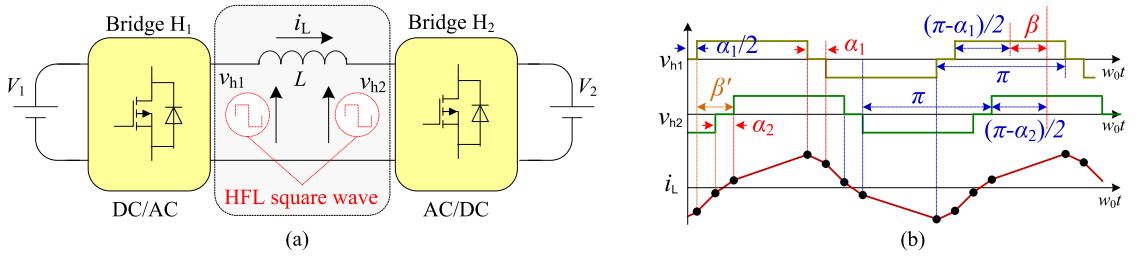

Fig. 1. (a) Equivalent circuit of DAB. (b) Unified phase-shift control principle.

H_1 and H_2, respectively; i_L is the HFL current. Note that V_2 and v_{h2} are the equivalent voltages in V_1 side.

All the PS control methods (such as SPS, EPS, DPS, etc.) proposed in previous literatures can be described with a unified form as shown in Fig. 1(b). In the unified form, both the HFL voltages contain three PS angles: α_1, α_2, and β. α_1 and α_2 are the PS angles caused by adjusting the driving pulses of the diagonal switches within the bridges H_1 and H_2; β is the PS angle caused by adjusting the driving pulses of the same switches between the bridges H_1 and H_2. SPS, EPS, and DPS can be taken as special cases of the unified form, such as the SPS control can be achieved when $\alpha_1 = \alpha_2 = 0$, the EPS control can be achieved when $\alpha_1 = 0$ or $\alpha_2 = 0$, the DPS control can be achieved when $\alpha_1 = \alpha_2$.

Note that the definition of β in this letter not only indicate the PS angle of the driving pulses of the same switches between the bridges H_1 and H_2, but also indicate the PS angle of the HFL voltages v_{h1} and v_{h2}, which is different with the outer PS angle β' defined in the previous literatures [7]–[12]. In the subsequent analysis, it can be found that the outer PS angle $\beta = \beta' + (\alpha_1 + \alpha_2)/2$ has a more reasonable physical significance.

B. HFL Voltage and Current Characterization

The HFL voltages in Fig. 1 can be transformed universally based on Fourier series, as follows:

$$\begin{cases} v_{h1}(t) = \displaystyle\sum_{n=1,3,5,\ldots} \frac{4V_1}{n\pi} \cos\left(n\frac{\alpha_1}{2}\right) \sin(nw_0 t) \\ v_{h2}(t) = \displaystyle\sum_{n=1,3,5,\ldots} \frac{4V_2}{n\pi} \cos\left(n\frac{\alpha_2}{2}\right) \sin[n(w_0 t - \beta)]. \end{cases} \tag{1}$$

From Fig. 1(a), the DAB can be equivalent to two ac voltages connected to both sides of an inductor, we have

$$i(t) - i(0) = \int_0^t \frac{v_{h1}(t) - v_{h2}(t)}{L}\, dt. \tag{2}$$

Considering the symmetry of DAB in one switching cycle, and the average current of the inductors over one switching period should be zero in steady state, we have

$$i\left(\frac{\pi}{w_0}\right) = -i(0) \tag{3}$$

where $w_0 = 2\pi f_s$ is the angular frequency and f_s is the switching frequency.

From (1)–(3), it can be derived

$$i(t) = \sum_{n=1,3,5,\ldots} \frac{4}{n^2\pi w_0 L} \sqrt{A^2 + B^2} \sin\left(nw_0 t + \arctan\frac{A}{B}\right) \tag{4}$$

where

$$\begin{cases} A = V_2 \cos\left(n\dfrac{\alpha_2}{2}\right)\cos(n\beta) - V_1 \cos\left(n\dfrac{\alpha_1}{2}\right) \\ B = V_2 \cos\left(n\dfrac{\alpha_2}{2}\right)\sin(n\beta). \end{cases} \tag{5}$$

According to the analysis above, except the fundamental wave, there are odd harmonics in all the HFL voltages and currents. The root mean square (RMS) values can be derived from

$$\begin{cases} U_{h1\mathrm{rms}} = \sqrt{\displaystyle\sum_{n=1,3,5,\ldots} U_{h1n}^2} \\ \qquad\qquad = \sqrt{\displaystyle\sum_{n=1,3,5,\ldots} \left[\frac{2\sqrt{2}V_1}{n\pi}\cos(n\frac{\alpha_1}{2})\right]^2} \\ U_{h2\mathrm{rms}} = \sqrt{\displaystyle\sum_{n=1,3,5,\ldots} U_{h2n}^2} \\ \qquad\qquad = \sqrt{\displaystyle\sum_{n=1,3,5,\ldots} \left[\frac{2\sqrt{2}V_2}{n\pi}\cos(n\frac{\alpha_2}{2})\right]^2} \\ I_{\mathrm{rms}} = \sqrt{\displaystyle\sum_{n=1,3,5,\ldots} I_n^2} \\ \qquad\qquad = \sqrt{\displaystyle\sum_{n=1,3,5,\ldots} \left[\frac{2\sqrt{2}}{n^2\pi w_0 L}\sqrt{A^2+B^2}\right]^2}. \end{cases} \tag{6}$$

C. HFL Active Power Characterization

The average power of DAB during one switching period can be described as

$$P = \frac{1}{T}\int_0^T v_{h1}(t) i(t) dt \tag{7}$$

where $T = 1/f_s$ is the switching period.

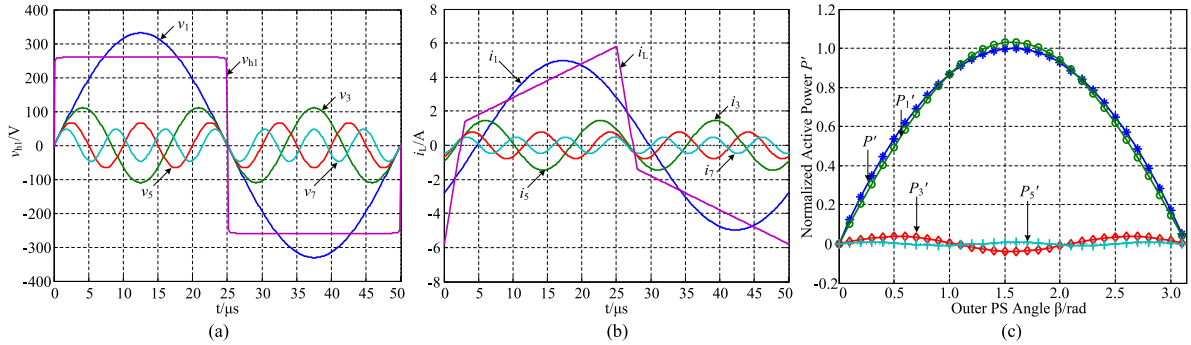

Fig. 2. Curves of different components of HFL electrical quantities under SPS modulation. (a) HFL voltage. (b) HFL current. (c) Active power.

From (1), (4), and (7), we have

$$P = \frac{1}{T}\int_0^T \sum_{n=1,3,5,\ldots} \frac{16V_1\sqrt{A^2+B^2}}{n^3\pi^2 w_0 L}\cos\left(n\frac{\alpha_1}{2}\right) \times \sin(nw_0t)\sin\left(nw_0t+\arctan\frac{A}{B}\right)dt + \frac{1}{T}\int_0^T \sum_{m\neq n} \frac{16V_1\sqrt{A^2+B^2}}{mn^2\pi^2 w_0 L}\cos\left(m\frac{\alpha_1}{2}\right) \times \sin(mw_0t)\sin\left(nw_0t+\arctan\frac{A}{B}\right)dt. \quad (8)$$

According to the orthogonality of trigonometric function, the second integral expression in (8) is equal to zero due to $m \neq n$. The product of the two sinusoids with the same frequency in the first expression is

$$\sin(nw_0t)\sin\left(nw_0t+\arctan\frac{A}{B}\right) = \frac{1}{2}\left[\cos\left(\arctan\frac{A}{B}\right)-\cos\left(nw_0t+\frac{1}{2}\arctan\frac{A}{B}\right)\right]. \quad (9)$$

From (8) and (9), we have

$$P = \sum_{n=1,3,5,\ldots} \frac{8V_1V_2}{n^3\pi^2 w_0 L}\cos\left(n\frac{\alpha_1}{2}\right)\cos\left(n\frac{\alpha_2}{2}\right)\sin(n\beta). \quad (10)$$

In fact, if the active power caused by the HFL voltage and current with the same frequency in (1) and (4) is defined as P_n, we have

$$P_n = \frac{8V_1\sqrt{A^2+B^2}}{n^3\pi^2 w_0 L}\cos\left(n\frac{\alpha_1}{2}\right)\cos\left(-\arctan\frac{A}{B}\right) = \frac{8V_1V_2}{n^3\pi^2 w_0 L}\cos\left(n\frac{\alpha_1}{2}\right)\cos\left(n\frac{\alpha_2}{2}\right)\sin(n\beta). \quad (11)$$

From (10) and (11), we have

$$P = \sum_{n=1,3,5,\ldots} P_n. \quad (12)$$

From (12), the whole power of DAB is equal to the sum of the separated average caused by the HFL voltage and current with the same frequency.

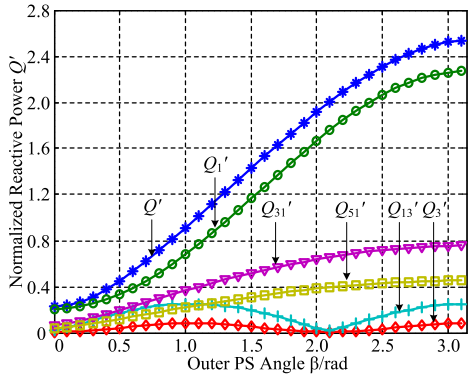

Fig. 3. Curves of the reactive power components varied with β.

According to the analysis above, Fig. 2 gives the curves of different components of HFL electrical quantities under SPS modulation. It can be seen that the HFL voltage and current composed by the odd components with different frequency, and the whole value are consistent with the waveforms achieved by the traditional piecewise linear method. In addition, the active power is just caused by the odd components with the same frequency. All the components of the active power are symmetric around the median axis $\pi/2$. In Fig. 3, all the power components are normalized with the value $P_N = V_1 * V_2/(8f_s * L)$, it can be seen that the maximum value of the whole power is 1, which is also consistent with the traditional model achieved by the traditional piecewise linear method.

Moreover, the fundamental components of all the HFL electrical quantities have the largest amplitude during all the components. Especially the fundamental power component is basically consistent with the whole power.

III. HFL Circulating Current Characterization

A. HFL Reactive Power Definition

As a dc–dc converter, the main function of DAB is to transfer active power. But due the existence of the ac HFL, there is a reactive power interaction among the HFL electrical quantities of DAB. In this letter, the reactive power of DAB is defined as the reactive power caused by the HFL voltage and current.

According to the analysis of Section II-B, all the HFL voltages and current of DAB are nonsinusoidal waves, and the reactive

power can be classified into two categories: 1) the reactive power caused by the voltage and current components with the same frequency; 2) the reactive power caused by the voltage and current components with the different frequency. From (1), (4), and (5), the reactive power of DAB with the first category can be derived

$$\begin{aligned} Q_{n=1,3,5\ldots} &= \frac{8V_1\sqrt{A^2+B^2}}{n^3\pi^2 w_0 L}\cos\left(n\frac{\alpha_1}{2}\right)\sin\left(-\arctan\frac{A}{B}\right) \\ &= \frac{8V_1\cos\left(n\frac{\alpha_1}{2}\right)}{n^3\pi^2 w_0 L}\left[V_1\cos\left(n\frac{\alpha_1}{2}\right)\right. \\ &\quad \left. - V_2\cos\left(n\frac{\alpha_2}{2}\right)\cos(n\beta)\right]. \end{aligned} \tag{13}$$

From (8) and (12), the voltage and current components with the different frequency do not produce the active power, so the reactive power of DAB with the second category can be derived

$$Q_{m\neq n} = U_{h1m}I_n = \frac{8V_1\cos(m\frac{\alpha_1}{2})}{mn^2\pi^2 w_0 L}\sqrt{A^2+B^2}. \tag{14}$$

The reactive power will cause the increase of the apparent power and the RMS current, and further increase power losses and the capacity of the DAB. That is why there are large circulating current in DAB and the efficiency is low. In this letter, the whole reactive power Q is defined as

$$Q = \sqrt{S^2 - P^2} \tag{15}$$

where S is the apparent power, we have

$$\begin{aligned} S &= U_{\mathrm{h1rms}}I_{\mathrm{rms}} \\ &= \sqrt{\sum_{n=1,3,5,\ldots} P_n^2 + \sum_{n=1,3,5,\ldots} Q_n^2 + \sum_{m\neq n=1,3,5,\ldots} Q_{m\neq n}^2}. \end{aligned} \tag{16}$$

Fig. 3 gives the curves of the reactive power components varied with β in SPS control. In Fig. 3, all the components are also normalized with $P_N = V_1 * V_2/(8f_s * L)$. It can be seen that the reactive power increases with the increase of β over the whole range [0, π]. From Fig. 2, there are always two symmetric angles β and π–β making the same active power, so the range [π/2, π] will make more reactive power than the range [0, π/2] for the same active power; therefore, we just analyze the condition of $0 \le \beta \le \pi/2$ in the following.

Moreover, the fundamental reactive power also has the largest amplitude during all the components and is basically consistent with the whole reactive power, respectively.

B. Universal Circulating Current Characterization

According to the analysis above, there is a reactive power interaction among the HFL electrical quantities of DAB. Using this reactive power interaction, the circulating current characteristic of DAB can be described accurately by HFL power factor (HFL-PF), as follows:

$$\lambda = \frac{P}{S}. \tag{17}$$

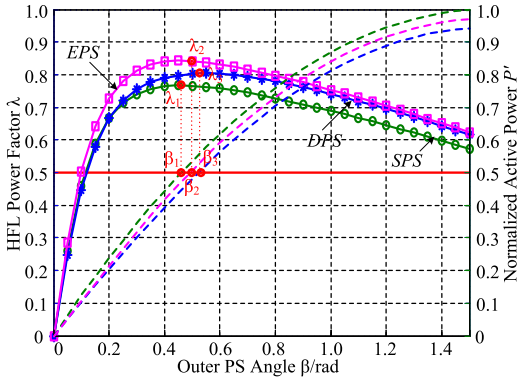

Fig. 4. Curves of the HFL-PF and active power varied with β under different control methods.

For a constant active power, the larger the circulating current the smaller the HFL-PF, and in turn, the smaller the circulating current, the larger the HFL-PF.

Fig. 4 gives the curves of the HFL-PF and active power varied with β under different control methods. It can be seen that the HFL-PF first increases and then decreases with the increase of β; there is a maximum point of HFL-PF. In SPS control, the PS angle β is used to control transmission power, so it cannot be used to find the optimal point of β. However, in the parameter design, the frequency f_s and inductance L are usually designed to ensure the PS angle operating in optimal range under the rated conditions. As for the PPS control methods, such as EPS and DPS, the outer PS angle β can be used to control transmission power and the inner PS angles α_1 and α_2 can be used to adjust the HFL-PF, further decreasing circulating current and increasing the efficiency. As shown in Fig. 4, compared to the SPS control, the EPS and DPS controls can produce higher HFL-PF with the same active power, and the HFL-PF will be different with the different inner PS angles. Therefore, to ensure the maximum HFL-PF, an optimal inner PS angle should be achieved.

IV. HFL Fundamental-Optimal Control Strategy

According to the above analysis, there are infinite components in the analytical model of active power P and apparent power S, and it is very difficult to achieve the optimal inner PS angles in a global solution in practice. However, from the analysis in Section IV-A, both the fundamental components of the active and reactive power have the largest proportion and are basically consistent with the whole active and reactive power. Therefore, to simplify the analysis, we can take fundamental component as an object to optimize the circulating current.

A. Fundamental-Optimal Model of Circulating Current

The HFL-PF defined in (17) is the global power factor of DAB, and the fundamental power factor λ_1 can be defined as

$$\begin{aligned} \lambda_1 &= \frac{P_1}{S_1} = \frac{P_1}{U_{h11}I_1} \\ &= \frac{V_2\cos(\frac{\alpha_2}{2})\sin(\beta)}{\sqrt{[V_1\cos(\frac{\alpha_1}{2}) - V_2\cos(\frac{\alpha_2}{2})\cos(\beta)]^2 + [V_2\cos(\frac{\alpha_2}{2})\sin(\beta)]^2}}. \end{aligned} \tag{18}$$

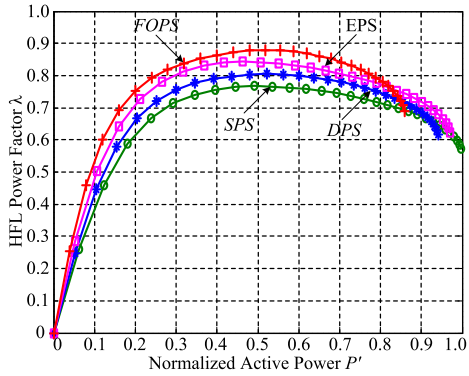

Fig. 5. Curves of the HFL-PF varied with the active power under different control methods.

From (18), λ_1 can reach to 1, where

$$V_1 \cos\left(\frac{\alpha_1}{2}\right) - V_2 \cos\left(\frac{\alpha_2}{2}\right)\cos(\beta) = 0. \tag{19}$$

Substituting (19) with (13), we have

$$Q_1 = 0. \tag{20}$$

From (20), the fundamental reactive power is eliminated. According to the analysis in Section III-B, to ensure the outer PS angle operating in optimal range under the rated conditions, the rated outer PS angle is usually designed with a small value. Therefore, (19) can be approximated to

$$V_1 \cos\left(\frac{\alpha_1}{2}\right) \approx V_2 \cos\left(\frac{\alpha_2}{2}\right). \tag{21}$$

From (1) and (21), the fundamental reactive power mainly relates to the amplitude difference between the fundamental components of the HFL ac voltages v_{h1} and v_{h2}. At this moment, the fundamental active power is

$$\begin{cases} P_1 = \dfrac{8V_2^2}{\pi^2 w_0 L}\cos^2(\dfrac{\alpha_2}{2})\sin(\beta) \leq \dfrac{8V_2^2}{\pi^2 w_0 L}\sin(\beta) \\ P_1 = \dfrac{8V_1^2}{\pi^2 w_0 L}\cos^2(\dfrac{\alpha_1}{2})\sin(\beta) \leq \dfrac{8V_1^2}{\pi^2 w_0 L}\sin(\beta). \end{cases} \tag{22}$$

In order to ensure the maximum capacity for the transmission power, $\cos(\alpha_1/2)$ and $\cos(\alpha_2/2)$ should be given a large value, from (22), we have

$$\begin{cases} \alpha_1 = 2\arccos\dfrac{V_2}{V_1}, \alpha_2 = 0 & V_1 \geq V_2 \\ \alpha_1 = 0, \alpha_2 = 2\arccos\frac{V_1}{V_2} & V_1 < V_2. \end{cases} \tag{23}$$

According to the analysis above, Fig. 5 gives the curves of the HFL-PF varied with the active power under different control methods. The control method based on fundamental-optimal model is defined as FOPS in Fig. 5. It can be seen that the FOPS has the highest HFL-PF during all the control methods.

B. Control Model of FOPS

Fig. 6 gives the control model of DAB based on FOPS control strategy. The outer PS angle is used to adjust the output voltage and power of DAB. The related control model is composed of a voltage controller and a current controller; the input of the voltage controller is the difference of the voltage reference value and the sensed output voltage, and the output is the current reference value; the current controller updates the outer PS angels according to the current reference value and the sensed current. The inner PS angles are used to adjust the circulating current of DAB. The related control model is composed of a circulating current controller, which updates the inner PS angles according to the online-sensed terminal voltages.

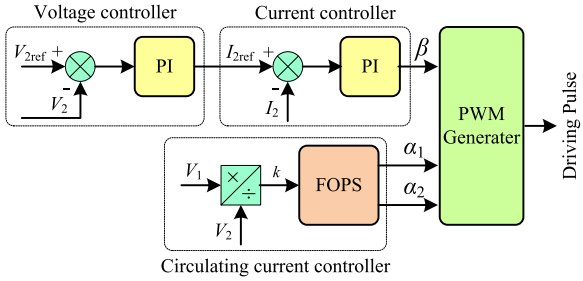

Fig. 6. Control model of DAB based on FOPS control strategy.

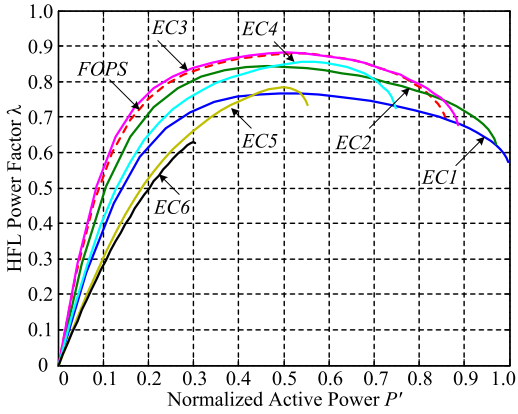

Fig. 7. Curves of the HFL-PF varied with the active power by enumeration method.

C. Discussion for the Optimization Effect of FOPS Control

According to the HFL characterization in Section IV, both the fundamental active and reactive powers have the greatest proportion in the whole power, so the FOPS is proposed.

Fig. 7 gives the curves of the HFL-PF varied with the active power by enumeration method. From Figs. 5 and 7, the FOPS control has the higher HFL-PF than SPS and other PPS controls in most cases. However, because the optimized object of FOPS is not the global circulating current, the PS angles decided by the FOPS are not global optimum solution. A special enumeration case (EC3) is shown in Fig. 7, where the circulating current under FOPS control is not the smallest.

However, because the global model is very complex, the global solution can be achieved by the enumeration method, but it is very difficult to achieve this by the analytical method,

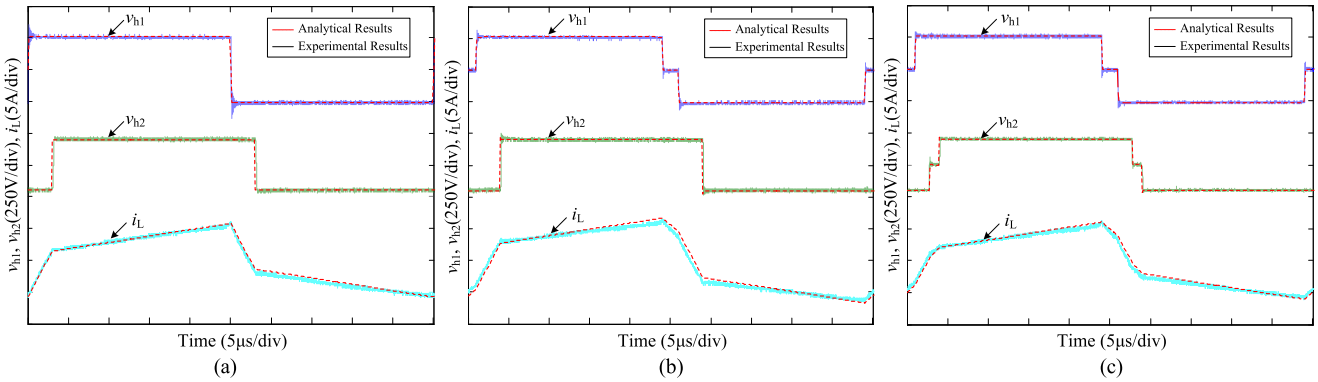

Fig. 8. Comparison waveforms of the HFL electrical quantities between the experimental and the analytically calculated results under different controls. (a) SPS control. (b) EPS control. (c) DPS control.

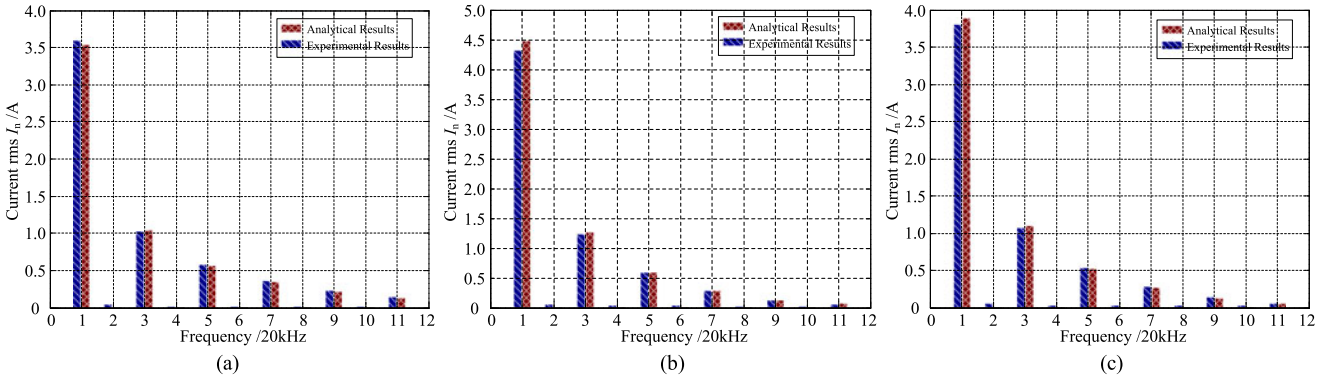

Fig. 9. Amplitude spectrum of HFL current between the experimental and the analytically calculated results under different controls. (a) SPS control. (b) EPS control. (c) DPS control.

which causes the implementing difficulties in practice. Therefore, the FOPS is still very simple and effective engineering optimal method in practice.

V. Experimental Verification

In order to verify the theoretical analysis in the letter, a 1-kW-DAB prototype is built. The main parameters are as follows: the series inductance $L = 200$ μH, the switching frequency $f_s = 20$ kHz; the dc terminal voltages $V_1 = 260$ V and $V_2 = 200$ V, the transformer ratio $N = 1.1{:}1$, that is, the equivalent voltage of V_2 in V_1 side is 220 V.

Fig. 8 shows the comparison waveforms of the HFL electrical quantities between the experimental and the analytically calculated results under different controls. It can be seen that the calculated results agree well with all the experimental results under different control methods, the HFL analytical model has the good universality.

Fig. 9 shows the amplitude spectrum of HFL current between the experimental and the analytically calculated results under different controls. It can be seen that the HFL current are composed mainly of odd components, and the fundamental component has the largest amplitude.

TABLE I
Comparison Results Under Different Controls

	Analytical Results			Experimental Results			
Electrical Quantity	SPS	EPS	DPS	SPS	EPS	DPS	Max Error
U_{1rms}	260	249	249	260	248	249	0.4%
I_{1rms}	3.73	4.68	4.06	3.78	4.52	3.97	3.4%
P	755	949	824	772	937	814	2.3%
S	970	1166	1013	983	1121	985	3.9%

Table I gives the comparison results of the HFL electrical quantities between the experiments and the analytically calculation under different controls. It shows that the analytically calculated results are very close to the experimental results, and the maximum error is less than 5%, which indicates that the proposed universal analysis method for the DAB is accurate enough to satisfy engineering requirements.

Fig. 10 shows the HFL-PF and efficiency of the DAB varied with the active power under different control methods. For different active power, the FOPS has the highest HFL-PF during all the control methods, which also improves the efficiency of the DAB. The experimental results coincide with the theoretical analysis.

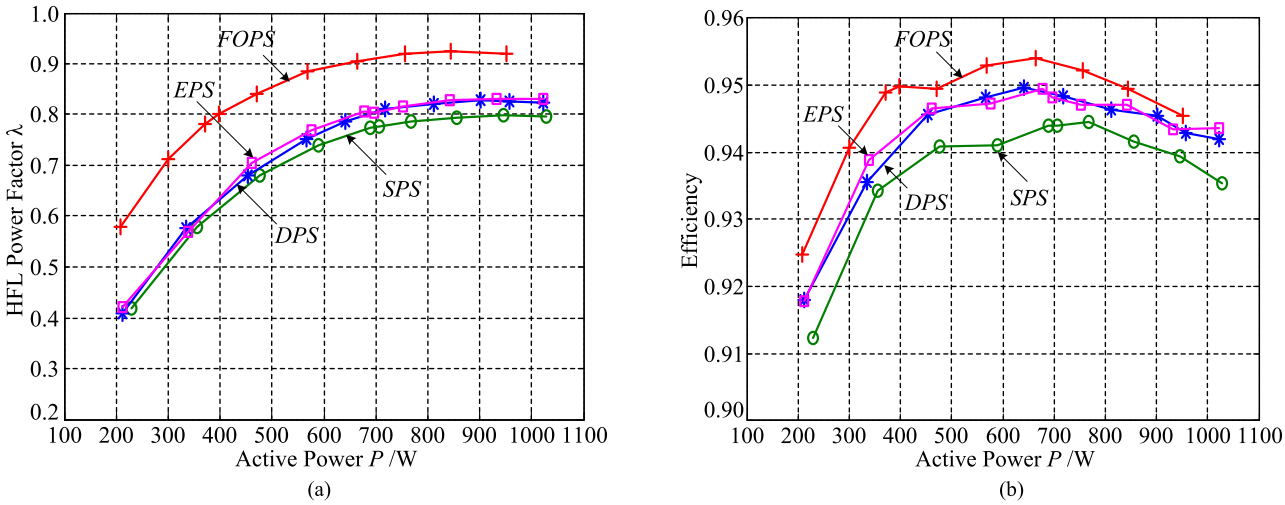

Fig. 10. HFL-PF and efficiency varied with the active power under different control methods. (a) HFL-PF. (b) Efficiency.

VI. Conclusion

Although the surface forms of various PPS controls are different, the essence of these controls is the same; by defining the outer PS angle appropriately, all the PS and PPS control methods can be descripted with a unified form. From the universal HFL characterization, both the HFL voltage and current are only composed of the odd components, and the active power is just caused by the components with the same frequency. Based on the universal characterization, a reactive power interaction among the HFL electrical quantities can be present, and the circulating current characteristic of DAB can be described accurately by the HFL power factor. As both the fundamental active and reactive power has the greatest proportion in the whole power, and the reactive and active power mainly relates to the amplitude and phase difference between the HFL ac voltages, respectively, the FOPS strategy can be used to decrease the circulating current and increase the efficiency. Although, the FOPS strategy is not the global optimum solution, it is a simple and effective engineering optimal method in practice which can be employed as a unified practical implement method for DAB.

References

[1] B. Zhao, Q. Song, W. Liu, and Y. Sun, "Overview of dual-active-bridge isolated bidirectional dc–dc converter for high-frequency-link power-conversion system," *IEEE Trans. Power Electron.*, vol. 29, no. 8, pp. 4091–4106, Aug. 2014.

[2] Y. Xie, J. Sun, and J. S. Freudenberg, "Power flow characterization of a bidirectional galvanically isolated high-power dc–dc converter over a wide operating range," *IEEE Trans. Power Electron.*, vol. 25, no. 1, pp. 54–66, Jan. 2010.

[3] D. Costinett, D. Maksimovic, and R. Zane, "Design and control for high efficiency in high step-down dual active bridge converters operating at high switching frequency," *IEEE Trans. Power Electron.*, vol. 28, no. 8, pp. 3931–3940, Aug. 2013.

[4] H. L. Chan, K. W. E. Cheng, and D. Sutanto, "Phase-shift controlled dc–dc converter with bidirectional power flow," *IEEE Elect. Power Appl.*, vol. 148, no. 2, pp. 193–201, Mar. 2001.

[5] H. Bai, Z. Nie, and C. Mi, "Experimental comparison of traditional phase-shift, dual-phase-shift, and model-based control of isolated bidirectional dc–dc converters," *IEEE Trans. Power Electron.*, vol. 25, no. 6, pp. 1444–1449, Jun. 2010.

[6] Z. Zhang, Z. Ouyang, O. C. Thomesen, and M. A. E. Andersen, "Analysis and design of a bidirectional isolated dc–dc converter for fuel cells and supercapacitors hybrid system," *IEEE Trans. Power Electron.*, vol. 27, no. 2, pp. 848–859, Feb. 2012.

[7] B. Zhao, Q. Yu, and W. Sun, "Extended-phase-shift control of isolated bidirectional dc–dc converter for power distribution in microgrid," *IEEE Trans. Power Electron.*, vol. 27, no. 11, pp. 4667–4680, Nov. 2012.

[8] H. Bai and C. Mi, "Eliminate reactive power and increase system efficiency of isolated bidirectional dual-active-bridge dc–dc converters using novel dual-phase-shift control," *IEEE Trans. Power Electron.*, vol. 23, no. 6, pp. 2905–2914, Nov. 2008.

[9] K. Wu, C. W. Silva, and W. G. Dunford, "Stability analysis of isolated bidirectional dual active full-bridge dc–dc converter with triple phase-shift control," *IEEE Trans. Power Electron.*, vol. 27, no. 4, pp. 2007–2017, Apr. 2012.

[10] A. K. Jain, "PWM control of dual active bridge: Comprehensive analysis and experimental verification," *IEEE Trans. Power Electron.*, vol. 26, no. 4, pp. 1215–1227, Apr. 2011.

[11] H. Zhou and A. M. Khambadkone, "Hybrid modulation for dual-active-bridge bidirectional converter with extended power range for ultracapacitor application," *IEEE Trans. Ind. Appl.*, vol. 45, no. 4, pp. 1434–1442, Jul./Aug. 2009.

[12] M. Kim, M. Rosekeit, S. K. Sul, and R. W. A. A. De Doncker, "A dual-phase–shift control strategy for dual-active-bridge dc–dc converter in wide voltage range," in *Proc. 8th IEEE Int. Conf. Power Electron. ECCE Asia*, Jeju, Korea, 2011, pp. 364–371.

[13] G. G. Oggier, G. O. Garcia, and A. R. Oliva, "Switching control strategy to minimize dual active bridge converter losses," *IEEE Trans. Power Electron.*, vol. 24, no. 7, pp. 1826–1838, Jul. 2009.

[14] B. Zhao, Q. Song, and W. Liu, "Efficiency characterization and optimization of isolated bidirectional dc-dc converter based on dual- phase-shift control for dc distribution application," *IEEE Trans. Power Electron.*, vol. 28, no. 4, pp. 1711–1727, Apr. 2013.